Three-phase bone scintigraphy for imaging osteoradionecrosis of the jaw

Constantin Lapa, Christian Linz, Christina Bluemel, Anja Mottok, Urs Mueller-Richter, Alexander Kuebler, Peter Schneider, Johannes Czernin, Andreas K. Buck, Ken Herrmann

Angaben zur Veröffentlichung / Publication details:

Lapa, Constantin, Christian Linz, Christina Bluemel, Anja Mottok, Urs Mueller-Richter, Alexander Kuebler, Peter Schneider, Johannes Czernin, Andreas K. Buck, and Ken Herrmann. 2014. "Three-phase bone scintigraphy for imaging osteoradionecrosis of the jaw." *Clinical Nuclear Medicine* 39 (1): 21–25. https://doi.org/10.1097/rlu.0000000000000296.

Three-Phase Bone Scintigraphy for Imaging Osteoradionecrosis of the Jaw

Constantin Lapa, MD, Christian Linz, MD,† Christina Bluemel, MD,* Anja Mottok, MD,‡ Urs Mueller-Richter, MD,† Alexander Kuebler, MD,† Peter Schneider, MD,* Johannes Czernin, MD,§ Andreas K. Buck, MD,* and Ken Herrmann, MD*§*

Abstract: This study evaluates the diagnostic utility of 3-phase bone scintigraphy for diagnosing osteoradionecrosis of the jaw (ORNJ).

Methods: Thirty-two consecutive patients with a history of radiation to the head and neck region (range, 62–70 Gy; mean, 68 Gy; median, 69 Gy) due to squamous cell cancer and suspected ORNJ underwent 3-phase bone scans after injection of 520 to 750 MBq of ^{99m}Tc-MPD. In addition to planar scans, tomographic images (SPECT) were acquired in the second phase and SPECT/CT images during the third phase. Histopathologic findings (n = 18) and clinical follow-up (n = 14) served as reference standard for osteoradionecrosis.

Results: The first, second, and third phases of planar images were rated positive in 18/32 patients (56.3%), 25/32 (78.1%), and 27/32 patients (84.4%), respectively. The late SPECT was positive in all patients (32/32, 100%), respectively. Histopathologic findings available in 18/32 patients (56.3%) confirmed ORNJ in all subjects. Acute inflammation was histologically proven in 18/18 specimens (100%) and additional chronic inflammation in 12/18 (66.7%). In 13/18 (72.2%) specimens, superinfection was evident histopathologically. A photopenic defect with surrounding hypermetabolism, a reported hallmark of ORJN, was found in less than 5%.

Conclusions: The predominant scintigraphic pattern of osteoradionecrosis includes increased bone mineralization phase in all patients. Central photopenia, reportedly a typical bone scan finding in bisphosphonate-induced osteonecrosis, was not characteristic for ORNJ. A differentiation of acute from chronic inflammatory processes was not possible.

Osteonecrosis of the jaw (ONJ) is a severe bone-related disorder that affects the mandible and/or the maxilla and is defined as exposed bone in the oral cavity with failure to heal.[1–3] Osteonecrosis of the jaw has recently gained clinical interest because its incidence has been rising as a result of more widespread (IV) bisphosphonate therapy. Although its pathogenesis is not fully understood, this phenomenon is now recognized as bisphosphonate-induced ONJ (BIONJ).[4] However, radiation therapy (RT) to the head and neck is also associated with ONJ. After radiation treatment, the incidence of osteoradionecrosis of the jaw (ORNJ) ranges from 2% to 22%. More recent reports suggested ORNJ rates of 8%.[5–7]

Osteoradionecrosis of the jaw has been believed to be directly linked to high radiation doses, whereas it rarely occurs at doses of less than 60 Gy.[8] Radiation induces vasculitis of small arteries resulting in tissue hypoxia.[9] Moreover, reduced bone turnover due to osteoclast damage[10,11] or bone cell damage due to fibroatrophic mechanisms, including endothelial dysfunction, free radicals, inflammation, microvascular thrombosis, fibrosis, and remodeling, and finally, bone and tissue necrosis have also been implicated in its pathogenesis.[12] As another striking feature, superimposed infection is frequently observed.[9,13] However, it is unknown whether this represents a primary or secondary phenomenon.

The diagnosis relies on visual inspection and clinical findings, such as pain due to nerve involvement (eg, inferior alveolar nerve) or signs of infection. Thus far, the contribution of noninvasive imaging to the diagnosis of ORNJ has not been addressed systematically.[2] Orthopantomography, cone beam CT, or CT are considered useful only when at least 30% of the bone mass is lost.[2,14,15]

Because functional alterations may occur before gross anatomic changes, bone scintigraphy may potentially detect ORNJ at an earlier time point than anatomical imaging modalities.[16] Osteonecrosis of the jaw presents as photopenic region surrounded by a hypermetabolic rim on bone scans, suggesting nonviable bone lesions with surrounding bone remodeling due to inflammatory changes or infection. However, this pattern has been observed mainly in patients with a history of bisphosphonate therapy. Little is known about bone scan findings in bisphosphonate naive patients.

The distinction between vital and nonvital bone is difficult. First, patients present before the sequestration of the larger parts of the nonviable bone, and thus, well-defined photopenic areas are infrequently seen. Second, smaller nonviable areas can be masked by surrounding infection.

We therefore aimed at investigating the performance of 3-phase bone scintigraphy to determine if the reported hallmark pattern of ONJ—central photopenia surrounded by increased tracer uptake—can be confirmed in patients with ORNJ.

PATIENTS AND METHODS

Because of the retrospective nature of the study, our institutional review board waived the requirement for informed consent.

Patients

Between 2006 and 2012, 32 patients with clinical suspicion of ORNJ (22 male and 10 female patients; mean age, 52.7 years; range, 31–80) underwent 3-phase bone scanning for further diagnostic workup. The indications for referral were exposed bone (81.3%), pain (31.3%), fistula (18.8%), and swelling (15.6%). Only patients who completed a 3-phase bone scan and additional SPECT or SPECT/CT scans during the second and third phase were included.

Three-Phase Bone Scintigraphy

Image acquisition started immediately after IV injection of 520 to 750 MBq ^{99m}Tc-labeled MDP (^{99m}Tc-MDP; mean activity, 696 MBq; radiation exposure, 3.0–4.3 mSv; mean, 4.0 mSv). Dynamic images of the primary region of interest (head with mandible and maxilla) were obtained in a 64 × 64 matrix in the anterior view at sixty 1-second frames for the first minute followed by

From the Departments of *Nuclear Medicine, and †Oral and Maxillofacial Plastic Surgery, University Hospital of Würzburg; ‡Institute of Pathology, University of Würzburg, Würzburg, Germany; and §Ahmanson Translational Imaging Division, Department of Molecular and Medical Pharmacology, David Geffen School of Medicine at University of California Los Angeles, Los Angeles, CA.

Constantin Lapa and Christian Linz contributed equally to the work.

Conflicts of interest and sources of funding: none declared.

Reprints: Constantin Lapa, MD, Department of Nuclear Medicine, University Hospital of Würzburg, Oberdürrbacherstr 6, D-97080 Würzburg, Germany. E-mail: lapa_c@klinik.uni-wuerzburg.de.

24 frames at 10 seconds (dynamic first phase). The blood-pool image (second phase) was obtained 5 minutes after injection using a 128 × 128 matrix (for 5 minutes). Additional SPECT images were performed for 10 minutes during the second phase.

Three hours after injection, whole-body scintigraphy was performed with static scanning of both the anterior and the posterior projections at a speed of 15 cm/min, using a dual-head γ-camera (e.cam; Siemens Healthcare, Erlangen, Germany). This was followed by a dedicated scintigram of the head.

Low-energy, high-resolution collimators were used. A 15% energy window was centered over the 140-keV photopeak of ^{99m}Tc. After the acquisition of the planar scans, a SPECT/CT emission/transmission study was performed (Symbia T2; Siemens Healthcare, Erlangen, Germany; 180-degree acquisition per detector, 128 × 128 matrix, 3-degree steps, and 20 s/frame).

Images were reconstructed using an iterative ordered subsets expectation maximization algorithm (Flash 3D: 0 Gaussian, 4 subsets, and 10 iterations), both with and without CT-based attenuation correction.

In 27/32 patients (84.4%), a low-dose CT was performed as part of SPECT/CT. The CT portion of the study was acquired using Care dose modulation (Siemens Healthcare, Erlangen, Germany) and 130 kV over 220 degrees, with a slice thickness of 0.5 cm and 0.8 seconds acquisition.

Transmission data were reconstructed using a B08s kernel to produce cross-sectional attenuation maps in which each pixel represented the attenuation of the imaged tissue. Transmission and emission images were fused on a dedicated nuclear medicine workstation (e.soft; Siemens Healthcare, Erlangen, Germany).

Image Analysis

Scans (planar, tomographic, and SPECT/CT hybrid scans) were interpreted independently by a team of 2 experienced nuclear medicine physicians (C.B. and C. Lapa) who were aware of the patients' clinical symptoms but who were blinded for the final histopathologic diagnosis.

A visual score dichotomizing the data was established as follows: the region of interest was considered negative if the uptake of the tracer was less than or equal to the contralateral site; a scan was defined as positive if tracer uptake was greater than on the contralateral side.

Images were read in the order of their acquisition starting with the dynamic images (first phase). Planar scans and SPECT were rated independently to assess foci, which might have been missed by planar imaging, but were detectable by tomographic scans (SPECT).

Overall, a positive region of interest in the late-phase (SPECT) images was sufficient for the diagnosis of ORNJ.

Reference Standards for the Diagnosis of ORNJ

Histopathologic findings were available in 18 of 32 patients (56.3%). For histologic examination, bone samples were fixed in 4% neutral-buffered formalin and subsequently decalcified for at least 72 hours in formic acid (Merck, Darmstadt, Germany). After paraffin embedding, 2-μm sections were cut, stained with hematoxylin-eosin, and reviewed by an experienced pathologist (AM) regarding the presence of necrosis, inflammation, and/or superinfection.

In cases presenting hyphae suspicious for fungal superinfection, an additional periodic acid–Schiff reaction was performed to confirm the presence of hyphae and/or yeast forms. The slides were assessed for the presence of osteonecrosis, inflammation, and secondary complications such as infection and osteomyelitis.

Histologic signs indicative for osteonecrosis included empty osteocytic lacunae and loss of hematopoietic cells and/or adipocytes in the partially fibrotic bone marrow spaces.

Samples were also assessed for the presence of secondary inflammatory changes. Acute inflammation was characterized by the presence of neutrophil granulocytes, whereas plasma cells and/or lymphocytes constituted chronic changes. Representative images were obtained using a DP26 camera (Olympus, Hamburg, Germany) and the cellSens Entry 1.5 Software version XV 3.5 (Olympus, Hamburg, Germany). To identify lesions with coexisting infection or superinfection, microbial cultures were performed in the available samples. These samples were tested for the presence of bacteria and/or fungi. In the remaining 14/32 patients (43.8%), no histopathologic finding was available. In this subgroup, clinical follow-up of at least 3 months served as reference. Persistence of exposed bone in the jaw confirmed the diagnosis of ORNJ in all of these 14 patients.

RESULTS

Patients

The mandible was the affected site in 27/32 (84.4%) patients, the maxilla in 2/32 (9.4%), and both in the remaining 3/32 (9.4%)

TABLE 1. Patients' Characteristics

Patients (n = 32)	Value	Cumulative Group Percentage
Age, y		
Range	31–80	—
Mean	52.7	—
Sex		
Male	22	68.7
Female	10	31.3
Tumor		
Oropharynx	9	28.1
Oral cavity	21	65.7
Hypopharynx	1	3.1
Submandibular gland	1	3.1
Tumor stage		
T1	8	25.0
T2	16	50.0
T3	2	6.3
T4	6	18.7
Osteoradionecrosis site		
Maxilla	2	6.3
Mandible	27	84.4
Both	3	12.8
Risk factors		
Alcohol	1	3.1
Nicotine	5	15.6
Alcohol + nicotine	17	53.1
None	3	9.4
Unknown	6	18.8
Time to manifestation after end of radiation, y		
Mean	3.2	—
Median	1.8	—
SD	3.1	—
Radiation dose, Gy		
Mean	68	—
Median	69	—
SD	3	—
Radiation period, d		
Mean	44	—
Median	42	—
SD	17	—

patients. All patients had a history of radiation to the head and neck region due to squamous cell cancer, with the most frequent primary site being the oral cavity (21/32, 65.6%), followed by the oropharynx (9/32, 28.1%). The remaining 2 patients had a history of cancer of the hypopharynx and the submandibular gland, respectively. Importantly, all but 1 patient were bisphosphonate naive.

All patients received radiation doses of 60 Gy or more to the tumor bed (range, 62–70 Gy; mean, 68 Gy; median, 69 Gy). Time from RT to development of clinical signs/symptoms averaged 39 months (range, 3.6–141.8 months). Patient characteristics are listed in Table 1.

Scintigraphic Findings

The first phase of the planar scans showed increased perfusion of the bone structure suspicious for ORNJ in 18/32 patients (56.3%). The blood-pool phase was rated positive in 25 patients (78.1%), whereas the late phase was interpreted as positive in 27 patients (84.4%). Late-phase SPECT was interpreted positive in all 32 patients and improved the diagnostic accuracy in 5 patients by delineating corresponding areas of bone necrosis not seen on planar scintigrams. An example is given in Figure 1, and a schematic presentation of bone scintigraphy results is given in Table 2.

CT as a Part of SPECT/CT

In 27 patients, a low-dose CT was performed in addition to the late-phase SPECT. Most of these patients' CT showed mixed sclerotic/lytic bone lesions. In addition, periostal thickening or irregularities of cortical bone were described. At least 1 of the features mentioned previously was present in 22/27 patients (81.5%). A sequestrum (24 mm each), the classic hallmark of osteonecrosis, was only identified in 2 patients (7.4%). CT was rated as nonsuspicious in 5 patients (18.5%).

TABLE 2. Bone Scintigraphy Findings

Imaging Phase	Positive Scan	Percentage, %
First phase	18/32	56.3
Second phase	25/32	78.1
Third phase	27/32	84.4
SPECT	32/32	100

Histological and Microbiological Findings

The histological examination results confirmed the diagnosis of osteonecrosis in all 18 patients in whom tissue samples were available. The affected bone showed lacunae characteristically devoid of osteocyte nuclei and loss of hematopoietic cells and/or adipocytes in the bone marrow spaces in the areas of necrosis. Interestingly, each sample showed also focal additional inflammation.

Acute inflammatory changes, characterized by the presence of neutrophil granulocytes, were observed in 18/18 patients. Additional chronic inflammatory cells were present in 12/18 (66.7%), whereas pure chronic infection could not be observed.

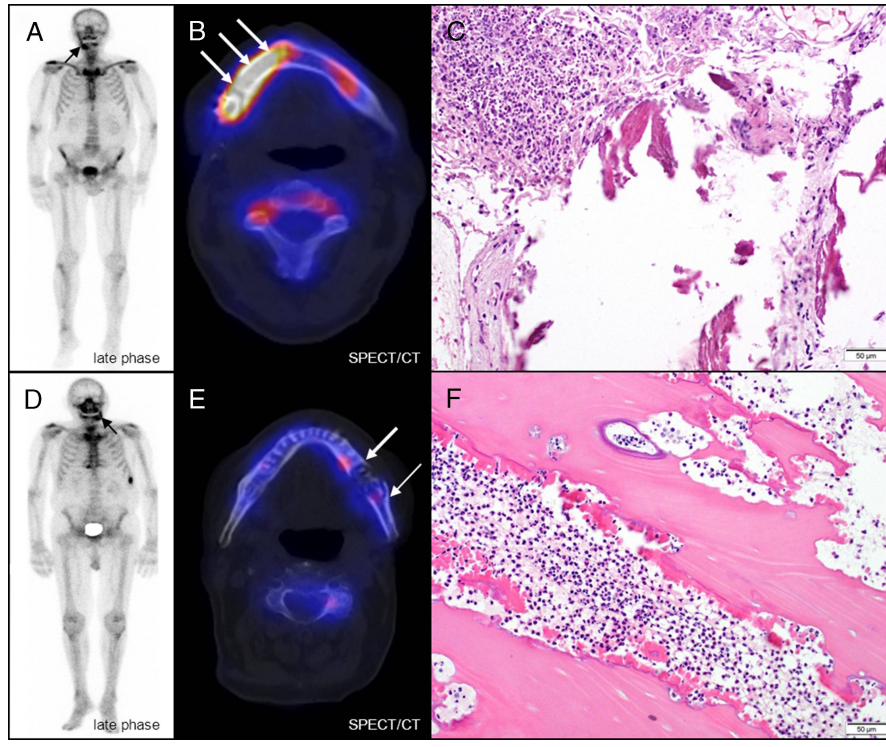

FIGURE 1. Two examples of ONJ and the different uptake pattern on bone scintigraphy. Both patients had a history of squamous cell cancer of the oral cavity and received radiation doses of 66 Gy to the primary tumor site, respectively. On planar imaging, both patients display increased tracer uptake at the site of suspected necrosis (A and D), which could be proven histologically afterward (C and F). Shown here are areas of necrotic bone with empty osteocytic lacunae and lack of osteoclasts. There are also numerous neutrophilic granulocytes as a sign of acute inflammation However, only patient 2 shows the generally postulated pattern of a central necrosis surrounded by reactively increased bone metabolism (E). Continuous uptake as shown in patient 1 (B) was observed much more frequently.

TABLE 3. Histological and Microbiological Findings

Patient	Osteonecrosis	Acute Inflammation	Chronic Inflammation	Superinfection
1	+	+	+	B
2	+	+	−	B
3	+	+	+	B
4	+	+	+	−
5	+	+	−	B/F
6	+	+	+	B/F
7	+	+	−	B
8	+	+	+	B/F
9	+	+	−	B
10	+	+	+	B
11	+	+	+	−
12	+	+	+	B
13	+	+	+	−
14	+	+	+	−
15	+	+	−	B
16	+	+	−	B/F
17	+	+	+	−
18	+	+	+	B

B indicates bacterial superinfection; F, fungal superinfection.

In 13/18 patients (72.2%), superinfection with mostly bacteria and fungi was observed. Dedicated microbiological workup revealed streptococci, staphylococci, and actinomyces as the most common microorganisms. With regard to fungal infections, *Candida* species were identified (Table 3). Neither the presence of acute or chronic inflammation within the jaw nor microbial infection correlated with increased perfusion or blood pool at the time of bone scintigraphy. Although acute inflammatory changes were found in every sample examined histologically, the perfusion phase of bone scintigraphy yielded positive results in just 11/18 (61.1%) patients (Fig. 2).

In the remaining 14 patients, clinical follow-up served as standard of reference. Here, the persistence or new development of exposed bone for a period longer than 12 weeks resulted in the diagnosis of ORNJ.

DISCUSSION

Osteoradionecrosis of the jaw is a severe complication after radiotherapy for head and neck cancer.[17] Although numerous studies have investigated the clinical value of imaging in the diagnosis of BIONJ, data on ORNJ are limited. To the best of our knowledge, this is the largest series of patients with clinical suspicion on ORNJ examined by 3-phase bone scintigraphy. The main finding of our study is a high sensitivity of 3-phase bone scans for detecting ORNJ. In our cohort, in all patients with histologically or clinically proven ORNJ, increased bone metabolism could be detected.

Our findings also reveal that tomographic imaging improves the diagnostic accuracy because hypermetabolic foci were diagnosed exclusively by SPECT in 15.6% of the patients. Second, anatomical correlation by low-dose CT improved colocalization of bone lesions. However, in 18.5% of patients, no anatomic alterations could be identified on low-dose CT images.

Recently published studies describe a necrotic core in more than 50% of ONJ patients, resulting in a central photopenic defect on bone

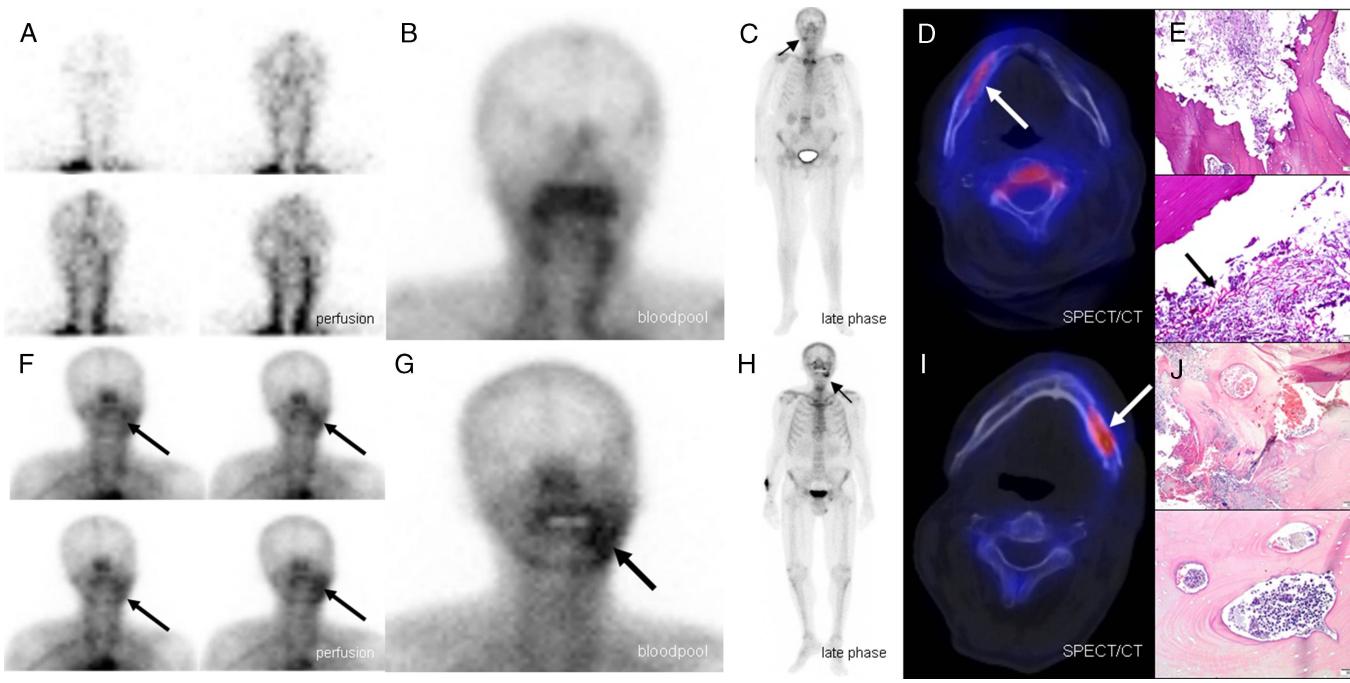

FIGURE 2. Two patients with a history of RT (patient 1, 68 Gy; patient 2, 66 Gy) due to squamous cell cancer of the oral cavity and histologically proven superinfected ORNJ. Although patient 1 (A–E) does not show increased perfusion (A) nor blood pool (B) and displays just moderately increased tracer uptake in late-phase imaging (C and D), pathologic finding reveals additional acute inflammatory changes with bacterial and fungal superinfection (E, periodic acid–Schiff reaction stain). In contrast, patient 2 (F–J) is positive in all 3 bone scan phases (F–I). Histological examination also confirms osteonecrosis with acute and chronic inflammation as well as microbial superinfection (E). Bone scintigraphy does not reliably distinguish between acute and/or chronic and/or no inflammatory changes.

scans surrounded by reactive, hypermetabolic tissue. However, in patients with ORNJ, this uptake pattern was only observed in 2 patients who presented with a large sequestrum of 24 mm each. In all other patients with ORNJ, necrosis presented as homogenously increased tracer uptake. A potential explanation could be the almost ubiquitous coexistence of inflammatory changes and/or superinfection in the areas of necrotic bone, which, due to limited spatial resolution, may mask small sequestra. Indeed, at least focal inflammation was present in every single bone sample that was examined histologically (n = 18). Microorganisms were observed in 72.2% (13/18) of patients, indicating that superimposed infections are common findings in ORNJ because of the relatively large amount of bacteria and fungi present in the oral flora.

It is commonly assumed that the different phases of bone scans provide diagnostic value. For instance, it has been suggested that acute and chronic infection/inflammation can be identified by a positive perfusion phase.[18] However, in our cohort, negative perfusion and blood-pool phases did not rule out acute infection. This might be due to radiation-induced changes in the blood supply of the jaw and therefore a variety of different reactions to inflammatory stimuli.[19] Nevertheless, the clinical value of perfusion and blood-pool studies as part of the 3-phase bone scan remains uncertain. In the current study, late-phase bone scans, including tomographic imaging of the jaw, were sufficient to confirm or rule out clinically suspected ORNJ.

Before translating our results into clinical routine, a number of limitations of this single-center trial have to be kept in mind. First, the study design was retrospective. Second, histological confirmation was not available in all patients. Third, imaging results of scintigraphy were not compared with other imaging modalities. Nevertheless, to our knowledge, our cohort comprises the largest group of histologically verified ORNJ.

Taken together, we hypothesize that all areas of increased bone metabolism in the jaw that are clinically suspicious for ORJN have to be strongly considered as osteoradionecrosis. This is supported by the fact that specificity is not a major concern in this setting as all patients are highly selected by the referring specialist.

CONCLUSIONS

Three-phase bone scintigraphy is a sensitive method to detect changes in bone metabolism after radiotherapy. Because of concomitant inflammatory and/or infectious processes, almost all cases of ORNJ present a homogenously increased bone metabolism without photopenia. Late-phase SPECT imaging is sufficient to make the diagnosis, because perfusion and blood pool do not offer reliable information on the presence of acute and/or chronic inflammatory changes.

REFERENCES

1. American Association of Oral and Maxillofacial Surgeons. American Association of Oral and Maxillofacial Surgeons position paper on bisphosphonate-related osteonecrosis of the jaws. *J Oral Maxillofac Surg*. 2007;65:369–376.
2. Chrcanovic BR, Reher P, Sousa AA, et al. Osteoradionecrosis of the jaws—a current overview—part 1: physiopathology and risk and predisposing factors. *J Oral Maxillofac Surg*. 2010;14:3–16.
3. Khosla S, Burr D, Cauley J, et al. Bisphosphonate-associated osteonecrosis of the jaw: report of a task force of the American Society for Bone and Mineral Research. *J Bone Miner Res*. 2007;22:1479–1491.
4. Watters AL, Hansen HJ, Williams T, et al. Intravenous bisphosphonate-related osteonecrosis of the jaw: long-term follow-up of 109 patients. *Oral Surg Oral Med Oral Pathol Oral Radiol*. 2013;115:192–200.
5. Jereczek-Fossa BA, Orecchia R. Radiotherapy-induced mandibular bone complications. *Cancer Treat Rev*. 2002;28:65–74.
6. Mendenhall WM. Mandibular osteoradionecrosis. *J Clin Oncol*. 2004;22:4867–4868.
7. Reuther T, Schuster T, Mende U, et al. Osteoradionecrosis of the jaws as a side effect of radiotherapy of head and neck tumour patients—a report of a thirty year retrospective review. *Int J Oral Maxillofac Surg*. 2003;32:289–295.
8. Goldwaser BR, Chuang SK, Kaban LB, et al. Risk factor assessment for the development of osteoradionecrosis. *J Oral Maxillofac Surg*. 2007;65:2311–2316.
9. Marx RE. Osteoradionecrosis: a new concept of its pathophysiology. *J Oral Maxillofac Surg*. 1983;41:283–288.
10. Al-Nawas B, Duschner H, Grotz KA. Early cellular alterations in bone after radiation therapy and its relation to osteoradionecrosis. *J Oral Maxillofac Surg*. 2004;62:1045.
11. Assael LA. New foundations in understanding osteonecrosis of the jaws. *J Oral Maxillofac Surg*. 2004;62:125–126.
12. Delanian S, Lefaix JL. The radiation-induced fibroatrophic process: therapeutic perspective via the antioxidant pathway. *Radiother Oncol*. 2004;73:119–131.
13. Store G, Boysen M. Mandibular access osteotomies in oral cancer. *ORL J Otorhinolaryngol Relat Spec*. 2005;67:326–330.
14. Ardran GM. Bone destruction not demonstrable by radiography. *Br J Radiol*. 1951;24:107–109.
15. Store G, Boysen M. Mandibular osteoradionecrosis: clinical behaviour and diagnostic aspects. *Clin Otolaryngol Allied Sci*. 2000;25:378–384.
16. Alexander JM. Radionuclide bone scanning in the diagnosis of lesions of the maxillofacial region. *J Oral Surg*. 1976;34:249–256.
17. Bagan JV, Jimenez Y, Hernandez S, et al. Osteonecrosis of the jaws by intravenous bisphosphonates and osteoradionecrosis: a comparative study. *Med Oral Patol Oral Cir Bucal*. 2009;14:e616–e619.
18. Prandini N, Lazzeri E, Rossi B, et al. Nuclear medicine imaging of bone infections. *Nucl Med Commun* 2006;27:633–644.
19. Dambrain R. The pathogenesis of osteoradionecrosis. *Rev Stomatol Chir Maxillofac*. 1993;94:140–147.